Investigation of microstructural and mechanical properties of partially hydrated Asbestos-Free fiber cement waste (AFFC) based concretes: Experimental study and predictive modeling

Harifidy Ranaivomanana, Nordine Leklou

Investigation of microstructural and mechanical properties of partially hydrated Asbestos-Free Fiber Cement waste (AFFC) based concretes: experimental study and predictive modeling

Harifidy RANAIVOMANANA[a*] ; Nordine LEKLOU[a]

[a] *GEM,UMR, CNRS 6163, IUT de Saint-Nazaire, Rue Michel Ange 44600*

[*]Corresponding author, email: Harifidy.Ranaivomanana@univ-nantes.fr

Highlights:

- Asbestos-Free Fiber Cement waste (AFFC) can be used as supplementary cementitious materials (SCM) in concrete formulations despite its low hydration potential.
- The incorporation of AFFC leads to a drop in total porosity, compressive strength and Young modulus due to the creation of capillary voids.
- An optimum dosage of AFFC equal to 10% was found. Below this value, a drop in gas permeability was observed because the created capillary voids are not interconnected enough to form percolation paths for gas flow.
- The mechanical performance evolution with time was predicted by using a modified Feret's law combined with Eurocode 2.
- The mechanical performances of concretes formulated with AFFC are comparable to that of concretes incorporating limestone filler.

1. ABSTRACT

Asbestos-Free Fiber Cement waste (AFFC) was tested in this study as supplementary cementitious materials (SCM) in concrete formulations. The incorporation of AFFC leads to a drop in total porosity, compressive strength and Young modulus due to the creation of capillary voids. The optimum dosage of AFFC is 10%. Below this value, the created capillary voids are not interconnected enough to form percolation paths for gas flow. A modified Feret's law combined with Eurocode 2 was proposed to predict the mechanical performance evolution with time. Finally, comparative tests between the performance of AFFC and limestone filler as SCM were also achieved.

Keywords: *Asbestos Free Fiber Cement, waste, microstructure, mechanical properties, permeability, porosity, modeling*

2. INTRODUCTION

The use of mineral fines as partial substitution of cement in concrete manufacturing presents several technical, economic and environmental advantages. These fines, also known as supplementary cementitious materials (SCMs), constitute a major alternative to reduce overall economic and environmental costs associated with the use of Portland cement **[1-5]**. Nowadays, SCMs are widely used in concrete either in blended cements (binary, ternary and even quaternary binder) or incorporated separately to the concrete mix. They have become an integral component of high strength, high performance and self-compacting concrete mix design. These materials may be quarry materials, industrial wastes or byproducts or products requiring less energy for their manufacturing. In addition to the economical and environmental benefits they induce, SCMs have the ability to interact with Portland cement **[6]**, reinforcing certain properties of the binder, such as the reactivity at early-age **[7]**, the mechanical strength development **[8]** and the long-term durability **[6; 9-12]**. It is also worth specifying that in addition to the use of SCMs, the incorporation of recycled aggregates in concrete formulations **[5; 13]** may represent an interesting solution from an environmental point of view.

Among the various existing SCMs, limestone filler (LF), fly ash (FA) and ground granulated blast furnace slag (GGBFS) are commonly used. The presence of LF generally increase early strength, enable to control the bleeding in concrete with low cement content, and reduce the sensibility to the lack of curing. Furthermore, LF acts as the crystallization nucleus for the precipitation of CH. These simultaneous effects produce an acceleration of the hydration of cement grains **[14].** FA and GGBFS, combined with cement in the proper proportion, participate to the strength development and durability, through their pozzolanic activity **[15; 16]**. The incorporation of FA and GGBFS in concrete is also a very efficient way to valorize those industrial by products.

Following this underlying trend in the research on more environmentally-friendly concrete, the recycling of other types of industrial byproducts as SCMs in concrete has been studied: amorphous silica **[17]**; rice husk **[18; 19]**, fly and scrubber-ash from an MSWI **[20]**; ceramic tile polishing residues **[21],** photovoltaic's silica-rich waste sludge **[22]**. In a similar context, the present study focuses on the potential valorization of asbestos-free fiber-cement (AFFC) as SCMs in concrete.

AFFC is a composite material made from cement, cellulose fibers, admixtures and water. Each year, the cutting of fiber-cement panels during the production process generated several hundreds of tons of waste **[23]**. These wastes contain a high dosage of unhydrated cement whose hydraulic activity could be exploited in mortar or concrete manufacturing.

Indeed, a recent study **[24],** Bouharoun et al. demonstrated that mortars incorporating AFFC ground between 80 and 100 microns, showed compressive strengths very similar to those measured on mortars prepared with LF, for a given substitution rate of cement (5 and 20%). A drop in mechanical properties was only observed for the coarser fraction of AFFC, with majority of particles ranging between 35 and 120 microns.

In the current research work, we investigate the microstructural and mechanical properties of AFFC based concretes in order to optimize the dosage of AFFC as SCM. In this purpose, water porosity measurements combined with gas permeability tests are performed to characterize the microstructure while Young modulus and compressive strength measurements are performed to characterize the evolution of mechanical properties. Finally, for the purpose of evaluating the effectiveness of AFFC as SCM and as performed by Bouharoun et al. **[24]**, comparative tests with limestone filler based concretes are also achieved. Moreover, based on experimental compressive strength values, a modification of Feret's law **[25]** is proposed to predict the mechanical performance of AFFC based concretes at 28 days.

3. MATERIALS AND MIXTURES

3.1 Materials

3.1.1 Cement

The cement used in this study was a CEM I 52.5 R, in accordance with **European standard [26]** from Saint Pierre La Cour plant (France). Its density was 3160 kg/m^3 and its Blaine fineness of 440 m^2/kg. The chemical composition of the cement is given in **Table 1**. Application of Bogue's formulas to the chemical composition of the cement gave the following mass distribution of the main phases: 61% of C_3S, 15% of C_2S, 8% of C_3A and 10% of C_4AF.

Table 1. *Chemical composition of cement (mass %)*

Cement	Massic content (%)
SiO_2	20.07
Al_2O_3	4.86
Fe_2O_3	3.07
CaO	64.25
MgO	0.95
SO_3	3.55
K_2O	1.00
Na_2O	0.20
Na_2O_{eq}	0.85

3.1.2 Sand and aggregates

Siliceous sand of Loire (France) was used for the manufacture of concrete. The particle size of the sand was between 0.08 mm and 6.3 mm, the density of the sand was 2580 kg/m^3.

The aggregates used are the crushed aggregates of 10/20 dimensions, coming from the career of Clarté at Missillac, France. The aggregates density is 2600 kg/m^3 and the water content is 1.05%.

The particle size distribution analysis of the sand and aggregates are given in **Figure 1**.

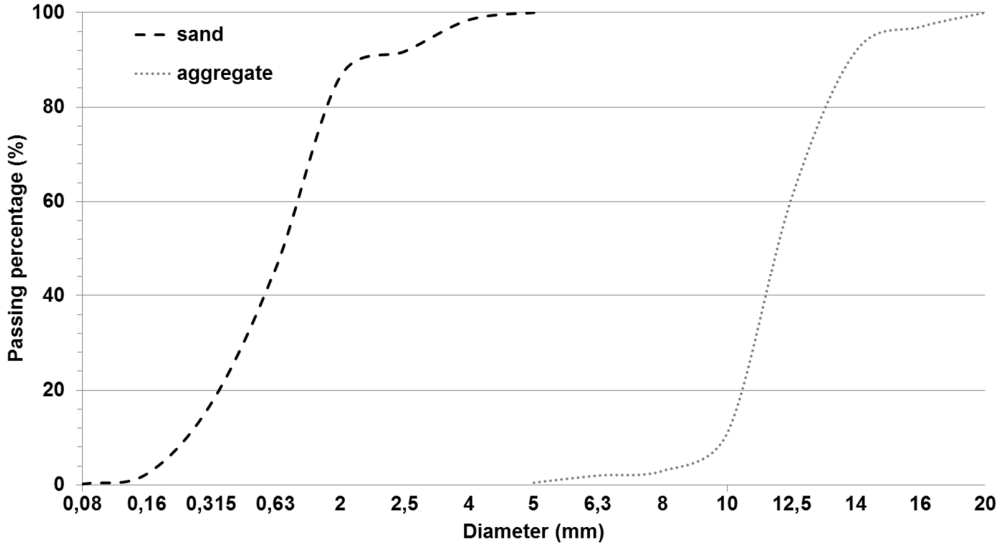

Figure 1. *Granulometric analysis of sand and aggregates*

3.1.3 Limestone filler

The LF used was a BETOCARB P2, produced at Erbray's plant (France), its $CaCO_3$ content was 97.30%. This limestone filler was characterized by a Blaine fineness of 397 m^2/kg, an absolute density of 2710 kg/m^3 and a water content of 0.1%.

3.1.4 Fiber-cement

The fiber-cement is a composite material made from cement (70 to 80%), cellulose fibers (5 to 10%), admixtures and water. Its density was 2230 kg/m^3.Considering the low dosage of used water, a significant amount of cement remains at the anhydrous state in the final material. The fiber-cement could therefore present a hydraulic potential, favorable to the development of cement mortar performances. Wastes of fiber-cement studied are in the form of flat and long thin slab with a few millimeters thick and several centimeters long (**Figure 2**).

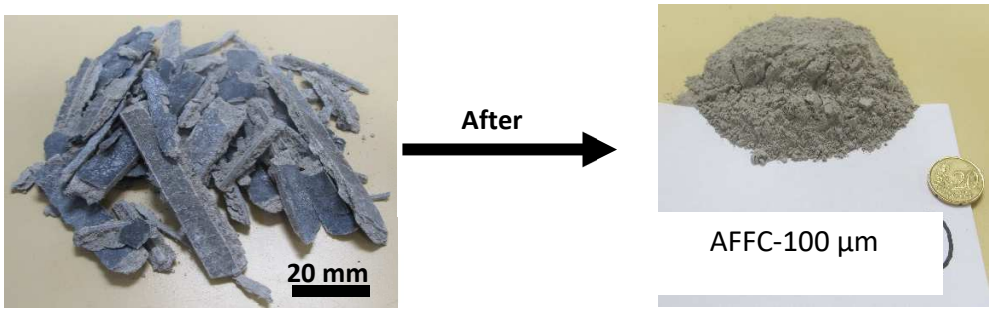

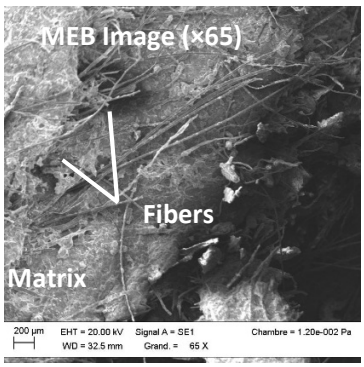

***Figure 2**. Fiber-cement wastes at raw state and after mechanical treatment (grinding and sieving) (AFFC-100 µm)*

They were initially ground to increase the contact surface between water and non-hydrated cement particles. Then, they were sieved on a column of sieves (100 µm) in order to obtain particle sizes, between 80 and 100 µm (denoted AFFC-100 µm).

The water content, the specific surface, the absolute density and the melting temperature **[27]** of the different ground fiber-cement grades, measured by pycnometry, are given in **Table 2**.

***Table 2.** Physical characteristics of fiber-cement*

Water content (%)	2.3
Density (kg/m^3)	2 230
Specific surface (cm^2/g)	4833
Melting Temperature (°C)	> 150

The particle size distributions of cement, fiber-cement and limestone filler measured using Laser granulometry are shown in **Figure 3**.

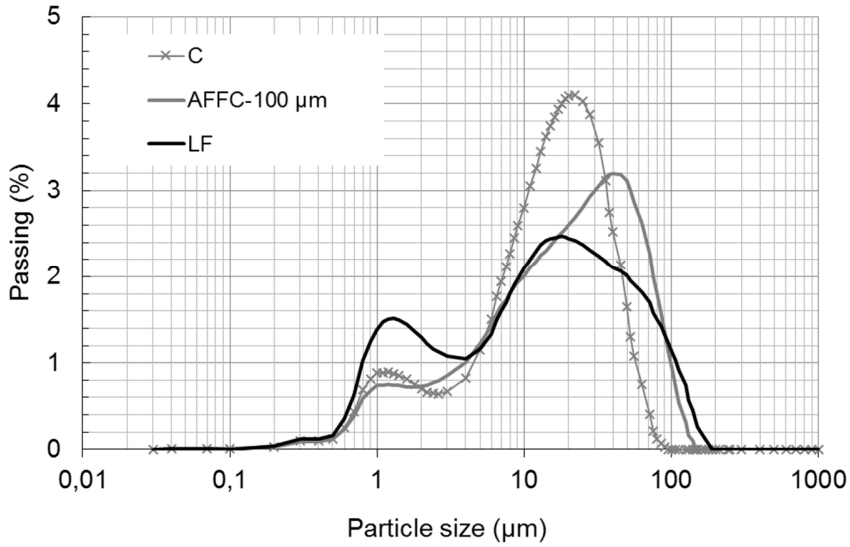

***Figure 3**. Size distribution of Portland cement (C), limestone filler (LF) and fiber-cement (AFFC-100 µm)*

The fractions of the different size classes are summarized in **Table 3**. The key point that emerged from these results was a greater fineness of limestone filler compared to that of cement and fiber-cement.

***Table 3.** Particle size classes of Portland cement (C), limestone filler (LF) and fiber-cement (AFFC-100 µm)*

	C	LF	AFFC-100 µm
90% of particles with Ø inferior or equal to	37.4 µm	66.0 µm	63.0 µm
50% of particles with Ø inferior or equal to	14.3 µm	13.5 µm	18.7 µm
10% of particles with Ø inferior or equal to	1.6 µm	1.2 µm	1.8 µm

3.2 Concretes

Seven concrete compositions made and mixed with a water/binder mass ratio (W/B) near 0.6 and an optimum binder to concrete volume ratio corresponding to a minimum value of the porosity related to the granular skeleton. This optimum volume ratio, noted as V_{FO} (L/m^3), is estimated from the following relationship (equation 1) derived from Dreux-Gorisse method **[28; 29]** and proposed by **[30]:**

$$V_{FO} = \frac{210}{\sqrt[5]{D}} + K \qquad (1)$$

Where :

D (mm) is the maximum size of coarse aggregate (14 mm).

K is a coefficient which depends corrective term which depends on the cement content, the clamping effectiveness, the rolled or crushed aggregates shape (the sand influence is especially preponderant) and also on the sand fineness modulus. K is equal to 5 for concretes used for making reinforced concrete elements with a reinforcement ratio not exceeding 80 kg/m^3.

The formulation objective is to obtain for fresh formulation a slump between 14 and 16 cm. In this paper, the term "binder" indicates the cement, used alone in the case of the ordinary concrete (OC), or the binary mixture of cement and fiber-cement (CAFFC-5%, CAFFC-10% and CAFFC-20 %,) or the binary mixture of cement and limestone filler (CLF-5%, CLF-10% and CLF-20%). The binary binders were made by substituting 5, 10 or 20% of cement mass by fiber-cement or limestone filler. The compositions of the concretes are given in **Table 4.**

Table 4*. Composition parameters, density at fresh state and the slump of the different concrete (the indicated ratios are mass ratios, OC: 100% of cement; CAFFC 5, CAFFC 10 and CAFFC 20: concrete with 5, 10 and 20 %, respectively, of cement substitution by the fiber cement; CLF 5, CLF 10 and CLF 20: concrete with 5, 10 and 20%, respectively, of cement substitution by the limestone filler.*

Concrete	OC	CAFFC 5	CAFFC 10	CAFFC 20	CLF 5	CLF 10	CLF 20
Cement (kg)	310	294.5	279	248	294.5	279	248
Sand (kg)	890.7	887.7	884.9	879.1	889.6	888.5	886.3
Aggregate (kg)	855.7	852.9	850.2	844.6	854.7	853.6	851.6
AFFC (kg)	0	15.5	31	62	0	0	0
LF (kg)	0	0	0	0	15.5	31	62
Water (kg)	180.44	181.7	184.63	184.5	185.3	183.6	173.3
W/L	0.58	0.59	0.59	0.59	0.59	0.59	0.56
Slump (cm)	16	14.7	15	16.5	14	14.7	13.8
Air content (%)	3.52	2.9	2.1	2.2	2	2	1.5
Experimental Density (kg/m^3)	2330	2440	2459.9	2390	2512.1	2521.8	2512.1
Theoretical density (kg/m^3)	2236.8	2232.3	2229.7	2218.2	2239.6	2235.7	2221.2

Slump tests using Abrahams Cone **[31]**, mechanical strength **[32]**, measurements of total shrinkage **[33]**, water-accessible porosity **[34]** and dynamic Young's modulus **[35]** were performed on concretes. The gas permeability was measured with CEMBUREAU method **[34]**. Two types of concrete specimens were produced: the cylinder specimens were poured in cardboard cylinder with 110 x 220 mm^2 of dimensions, and the cubic specimens, with 70 x 70 x 280 mm^3 dimensions, in metal molds with some of them being equipped with stainless steel studs for the measurement of total shrinkage. The properties of mixtures incorporating ground fiber-cement or limestone filler were then compared to those of the control concrete made with pure cement.

After pouring, the cylinder and cubic specimen were stored in a humidity chamber during 24 hours at 20 ± 1 °C and at a relative humidity above 90%. After 24 hours, the specimens were demolded. Those manufactured for mechanical tests were kept in the humidity chamber. The specimens dedicated to the measurement of total shrinkage and Young's modulus were kept in a room at 20 ± 1 °C and 50 ± 5 % of relative humidity.

4. EXPERIMENTAL METHODS

4.1 Dynamic Young's modulus and mechanical strengths at 14, 28 and 90 days

Dynamic Young's modulus was measured on the concrete specimens according to European standard **[35]**. Measurement consisted in determining the sample density and the fundamental transverse resonant frequency of concretes. This frequency was determined with an impulse excitation technique using a Grindosonic® device. The operation consisted in performing a slight elastic shock on the specimen and analyzing the phenomenon of transient vibration that follows. Then, the fundamental transverse resonant frequency was determined electronically. For each concrete, the determination of Young's modulus was performed on three specimens manufactured from the same mixture. The compressive strength was determined according to the procedure of European standard **[32].** Reported data for each concrete represent the average values obtained from three tests for compressive strength.

4.2 Water-accessible porosity

The open porosity of concretes was determined using a procedure based on that recommended by **[34].** Three specimens, with 110 x 50 mm² of dimensions, were tested for each concrete. Each sample was previously dried at 105°C to constant mass. It was stopped when the mass variation became lower than 0.05%. The sample was then saturated with water and under vacuum for 48 h. At the end of the saturation sequence, it was weighed and its volume was determined using hydrostatic weighing. The porosity P was then calculated using the following formula (equation 2):

$$P = \frac{M_{sat} - M_{dry}}{\rho_{water}.V} \quad (2)$$

Where:

M_{sat}: Mass of saturated concrete sample (g)

M_{dry}: Mass of dry sample (g)

V: Volume of sample (cm^3)

ρ_{water}: Density of water (g/cm^3)

For each concrete composition, two half-specimens were tested in order to calculate an average value of open porosity accessible to water.

4.3 Gas permeability

The permeability was important parameters determined the concrete durability. The CEMBUREAU method was used for identify the gas-transport properties of concrete. The residual gas permeability was determined using a procedure based on that recommended by **[34].** The permeability test was conducted on materials dried at 105°C and after specimens cooling. Before the permeability test, it is important that the material be in a homogeneous state regarding to water and thermal state. The tests are conducted essentially in steady state. Nitrogen is used as neutral percolation gas. The measurements were based on a "quasi permanent" flow rate of gas. For each pressure P, the corresponding apparent permeability (Ka) was measured by applying the law of Hagen-Poiseuille (8) which takes into account the compressibility of the fluid.

$$k_a = \frac{2 . P_a . Q . L . \mu}{A \left(P^2 - P_a^2\right)} \quad (m^2) \qquad (3)$$

P_a and P: are the pressure at the inlet and the outlet of the cell respectively, Q is the fluid flow, L and A are the width and the surface area of specimen respectively and μ is the nitrogen dynamic viscosity at 20°C (1.75×10^{-5} N s/m^2). For each concrete three samples were tested, each samples were 50 mm width and 110 mm diameter. The apparent residual permeability was obtained for air pressures between (0.05 and 0.3 MPa). After the determination of the apparent permeability at the fluid pressure (P), according to the method of "Klinkenberg", the intrinsic permeability "k_v" is obtained by plotting the curve of the apparent permeability as a function of the inverse of the average pressure "1/Pm" following to the equation (4).

$$k_a = k_v \left(1 + \frac{b^*}{P_m}\right) \quad (m^2) \qquad (4)$$

Where P_m is the gas pressure ($P_m = (P + P_a)/2$) and b* is the Klinkenberg coefficient.

k_v is the limiting value of gas permeability when the mean pressure P_m tends toward infinity. The intrinsic gas permeability "k_v" determined in Eq. (4) was depended on the degree of water humidity of the tested concrete without taking into account any drying process of the specimen before testing.

4.4 Thermogravimetric analysis

The thermogravimetric analysis (TGA) tests were performed by using a METTLER TOLEDO TGA/DSC1 with a balance accuracy of 0.1 µg. The dynamic heating ramp varied between 25°C and 1025°C with a heating rate of 5°C/min. The test was done under N_2 atmosphere. At the testing times (90 days), a 20 to 30 mg of pastes specimens cured at 20°C was crushed by using a pestle and mortar in order to obtain a particle size distribution lower than 0.4 µm. These pastes samples were then placed in a platinum

crucible. In this work, it should be noted that no processing or drying was made in order to avoid the hydrates instability **[36,37].**

5. RESULTS AND DISCUSSION

5.1 Water-accessible porosity results

The evolution of water porosity with the substitution rate of cement, for CAFCC and CLF formulations, are reported in **Figure 4**.

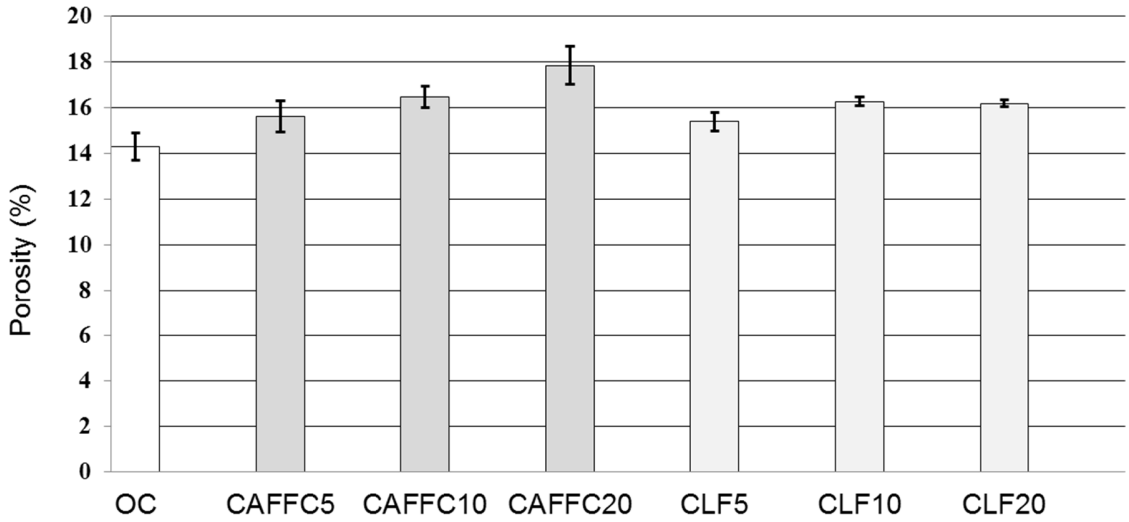

***Figure 4**. Evolution of water porosity with substitution rate of cement for CAFCC and CLF formulations*

For CAFCC formulations, the replacement of cement by AFCC leads to an increase in water porosity. Indeed, as mentioned above, concretes are formulated with a constant binder to concrete volume ratio, which corresponds to the optimum ratio given by equation 6. It means that the mass of binder involved in the formulation of a given volume of concrete decreases when increasing the substitution rate of cement, due to the drop in the density of the binder as recorded in **Table 5**.

***Table 5**. Evolution of binder density with substitution rate of cement*

Substitution rate (%)	**0**	**5**	**10**	**20**
CAFCC formulations				
Binder density (kg/m^3)	**3160.00**	**3091.53**	**3025.97**	**2902.85**
CLF formulations				
Binder density (kg/m^3)	**3160.00**	**3133.98**	**3058.43**	**3108.33**

This decrease in the mass of binder not only leads to a reduction in the mass of cement (replaced by AFFC) but also in that of water because of the constant water to binder mass ratio (W/B=0.6). Consequently, and given the low hydration potential of AFFC observed previously, the volume of cement hydration products for a given volume of concrete becomes lower when increasing the substitution rate of cement and results in the formation of more capillary voids which is responsible for the increase in the water porosity.

For CLF formulations, the replacement of cement by LF leads to an increase in water porosity up to a substitution rate of 10%. Given the constant volume ratio between the binder and the concrete mix as with AFCC formulations (optimum ratio), the mass of binder involved in the formulation of a given volume of concrete decreases too when increasing the substitution rate of cement, because of the drop in the density of the binder as recorded in Table 5. A lower volume of cement hydration products is thus formed for a given volume of concrete, resulting in the creation of more capillary voids. However, a slight decrease in water porosity is observed for substitution rates ranged between 10% and 20%. This refinement of the porous structure can be explained by the formation of monocarboaluminate produced by the transformation of monosulfoaluminate as a result of an excess of carbonate ions combined with a higher density of monocarboaluminate compared to that of monosulfoaluminate **[38]**. The presence of monocarboaluminate on CLF formulation with a substitution rate of 20% is confirmed by thermogravimetric analysis (**Figure 5**) combined with SEM observations (**Figure 6**). The morphology of concretes are characterized using scanning electron microscopy (SEM) EVO40 (Carl Zeiss®).

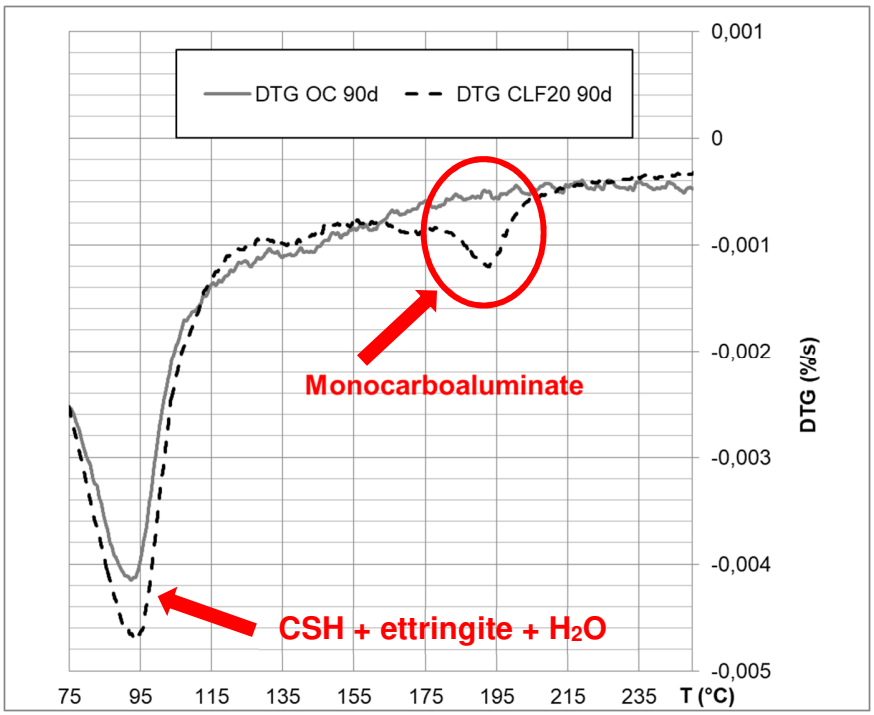

***Figure 5**. DTG Results of Reference Sample (OC) and CLF20 at the Age of 90 days*

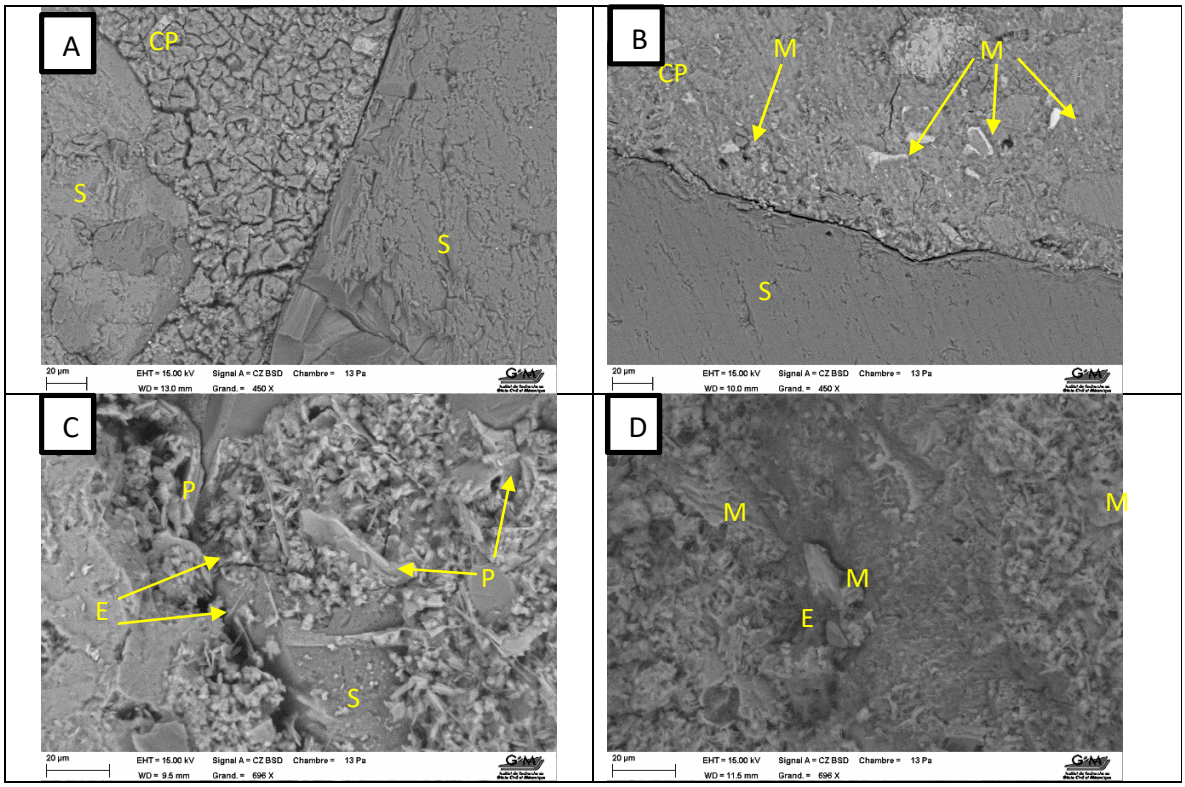

***Figure 6**. SEM image on "OC" (A & C) and "CLF20" (B & D) at 90 days (Low-Vacuum – x450 and x696). (CP: Cement Paste, S: Sand, P: Portlandite, E: Ettringite, M : Monocarboaluminate).*

Let us note that this transformation of monosulfoaluminate into monocarboaluminate was already observed experimentally by other researchers **[14;39]**. It is worth noting that the formation of monocarboaluminates could have been occurred even for substitution rates lower that 10%. However in that case, the impact of the presence of monocarboaluminates on the water porosity is probably compensated by the creation of capillary voids.

5.2 Gas permeability results

The evolution of gas permeability with the substitution rate of cement, for CAFCC and CLF formulations, are reported in **Figure 7**.

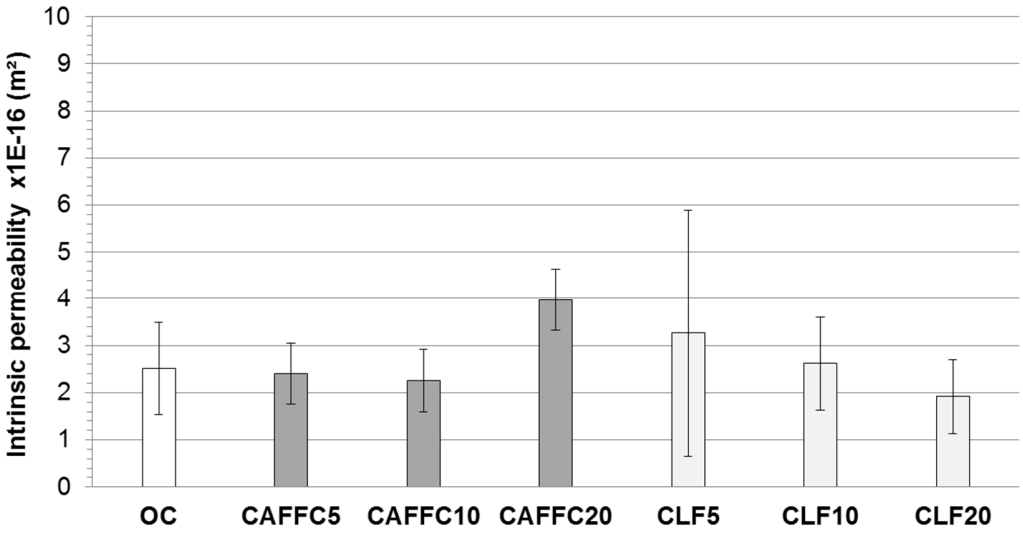

Figure 7*.Evolution of gas permeability with substitution rate of cement for CAFCC and CLF formulations*

Unlike water porosity evolution, the replacement of cement by AFCC first leads to a decrease in permeability for substitution rates of cement up to 10%. This observation can be explained by the fact that the interconnection of created capillary voids are strongly influenced by the partial substitution of the cement by AFFC with rates ranging from 0 to 10% despite the creation of porosity. Indeed, the created capillary voids are not interconnected enough to form percolation paths for gas flow. However, for higher rates of substitution, *i.e.* between 10% and 20%, it can be observed that water porosity and gas permeability of CAFCC formulations evolve in the same way. This would mean that beyond a threshold value of substitution rate (equal to 10%), the created capillary voids become increasingly interconnected, promoting the percolation of gas through the material. A schematic representation of the evolution of CAFCC microstructure is illustrated in **Figure 8a**.

For CLF formulations, the replacement of cement by LF first leads to an increase in permeability for substitution rates of cement up to 5% followed by a decrease for higher rates of substitution. This result is consistent with the formation of monocarboaluminates in CLF formulations, which are certainly responsible for the progressive reduction of the percolation paths. For substitution rates ranged between 5 and 10%, the drop in gas permeability is accompanied with an increase in water porosity due to the fact that the production of monocarboaluminates is compensated by the creation of capillary voids. These compensating effects become less pronounced from a threshold value of substitution rate (equal to 10%), for which water porosity and gas permeability evolve in the same way. A schematic representation of the evolution of CLF microstructure is illustrated in **Figure 8b**.

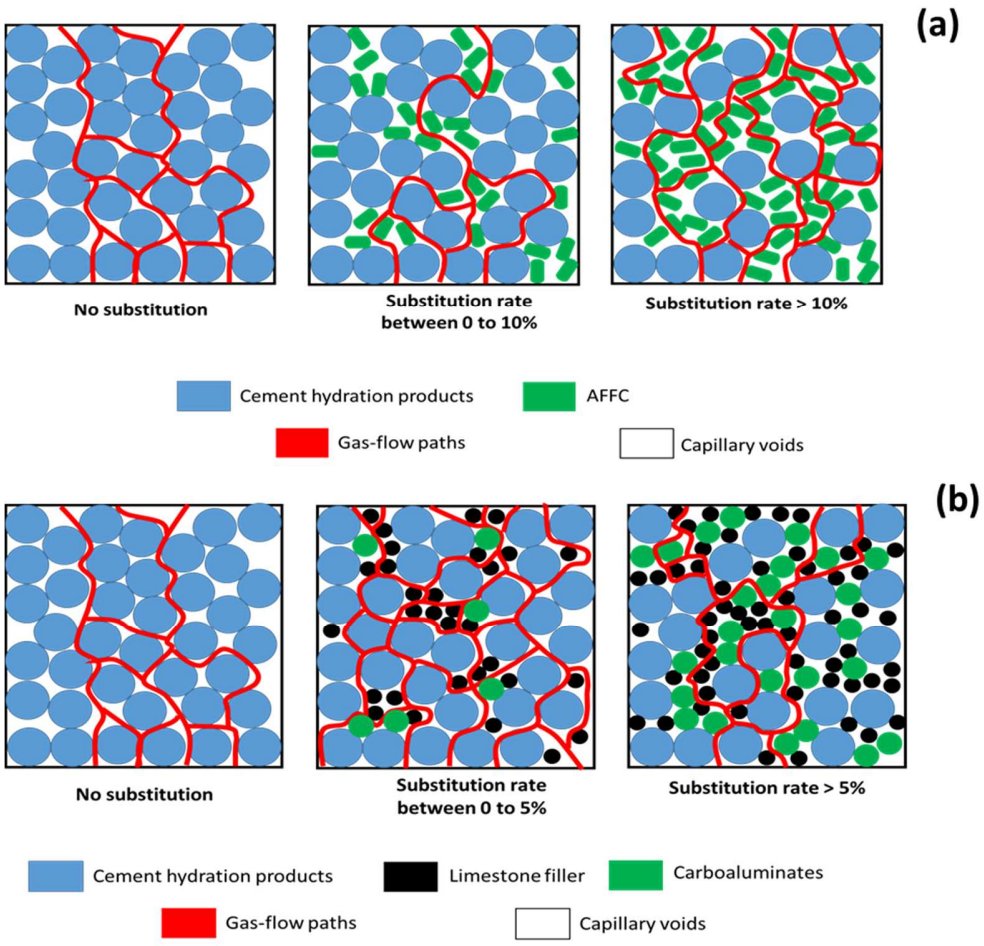

Figure 8. *.Schematic representation of the evolution of CAFFC microstructure (a) and CLF microstructure (b)*

5.3 Mechanical performance: compressive strength and Young modulus

The compressive strength and Young modulus at 14, 28 and 90 days respectively are presented depending on the incorporation rate (5, 10 and 20 %) of fiber-cement and limestone filler in **Figures 9 and 10**,

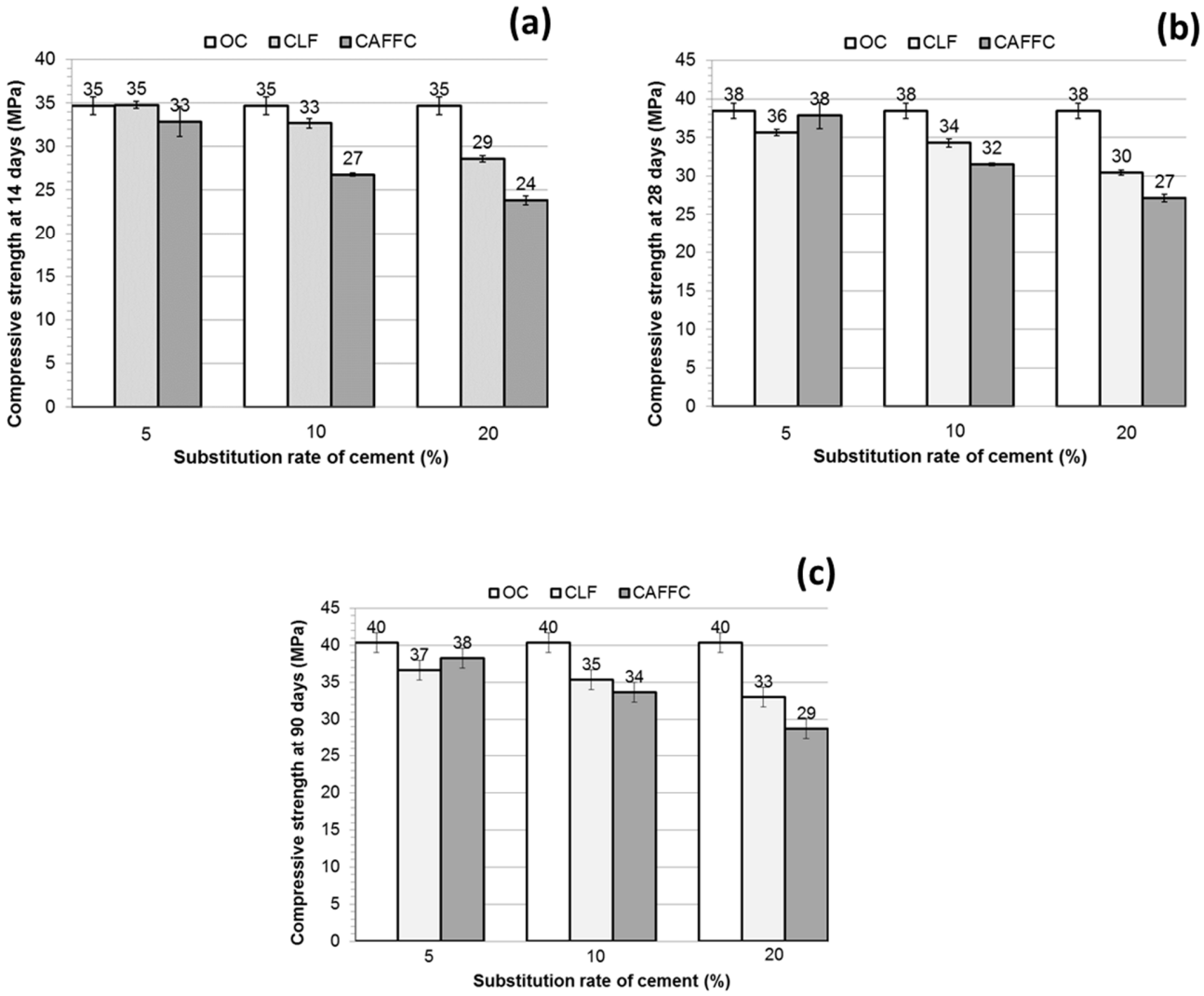

Figure 9*.Evolution of compressive strength at 14 days (a), at 28 days (b) and at 90 days (c) with substitution rate of cement for OC, CLF and CAFCC formulations*

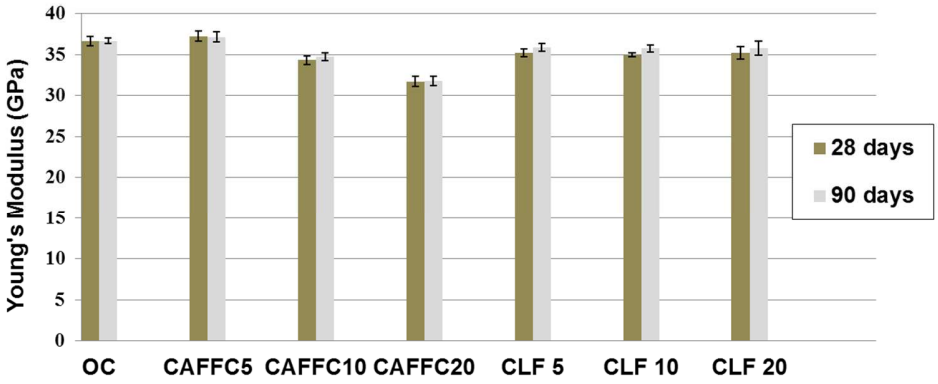

***Figure 10**. Evolution of Young modulus at 28 and 90 days with substitution rate of cement for OC, CLF and CAFCC formulations*

As previously observed by **[24]** on mortar samples, the partial replacement of cement with fiber-cement or limestone filler induces both a decrease in compressive strength and in Young modulus as the substitution rate of cement increases. The fraction of cellulose fibers present in the fiber-cement powder (**Figure 11**), lighter and less resistant to compression, was probably at the origin of this difference in performance.

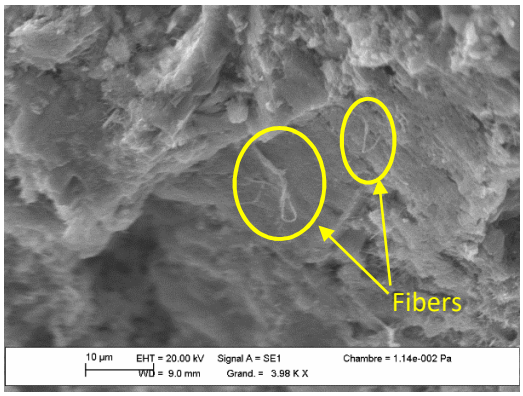

CAFFC 20% (X 3.98K)

***Figure 11**. SEM image of CAFCC 20% allowing to assess the distribution of the fibers and their relationships with the matrix taken by SEM in high vacuum mode (× 3.98 KX – 10µm).*

Let us however note a gain of **1 to 3 MPa** in compressive strength for both CAFCC and CLF formulations between 14 and 90 days. The reduction in compressive strength for CAFCC formulations is not a surprise given the creation of capillary voids induced by the lower Portland cement dosage as previously mentioned to explain water porosity and gas permeability results. For CLF formulations, the formation of monocarboaluminates does not contribute to improve the compressive strength despite the refinement of the porous structure **[39;40].** This result is probably due the low compressibility of monocarboaluminates as reported by **[41].**

6. ANALYTICAL MODELING

6.1 Presentation of Feret's model

As mentioned in introduction, a prediction of the compressive strength of concretes incorporating AFFC is also targeted in this study by using Feret's model which is the most well recognized strength equation relating compressive strength to concrete characteristics. Moreover, it is well-checked experimentally over a wide range of compressive strength values varying from 20 up to 100-150 MPa. The relation of Feret is written as follows in its most complete form:

$$f_{cm28} = \mathrm{G} \times \sigma_{L28} \times \left(\frac{v_b}{v_b+v_w+v_v}\right)^2 \quad (5)$$

Where

f_{cm28} (MPa) is the compressive strength at 28 days.

σ_{L28} (MPa) is the strength of the binder at 28 days. The term "binder" refers to the cement with or without additions.

v_b(m^3), v_w (m^3) and v_a(m^3) are the respective volumes of binder, water and entrained air, brought back to the volume of the concrete.

G is a coefficient depending on the type of the aggregates (G varies around 5 in general).

The volume of entrained air v_a can be determined experimentally or estimated from the following relationship proposed by **[30]**.

$$v_a = \frac{3\times v_b}{h+9} \times \frac{v_s}{v_s+v_g} \quad (6)$$

Where v_s (m^3) and v_g (m^3) are the respective volumes of sand and gravel brought back to the volume of the concrete.

The strength of the binder at 28 days σ_{L28} depends on that of the cement at the same age denoted as σ_{c28}.

$$\sigma_{L28} = \xi \times \sigma_{c28} \quad (7)$$

Where ξ is a coefficient which varies with the type of additions. For example, ξ=1 for an Ordinary Portland Cement (OPC) and is less than 1 for binders containing limestone fines or fly ash as additions **[26].** In the present study, a relationship between the coefficient ξ and the substitution rate of cement by AFFC is thus established.

Finally, the modified Feret's law equation proposed in this paper can be combined with an expression giving the development of compressive strength with time, such as proposed by Eurocode 2 **[42].**

$$f_{cm}(\mathrm{t}) = [\beta_{cc}(t)] \times f_{cm28} \quad (8)$$

Where $f_{cm}(t)$ is the mean compressive strength at age t days.

$$\beta_{cc}(\mathrm{t}) = \exp\left\{s\left[1-\left(\frac{28}{t}\right)^{0.5}\right]\right\} \quad (9)$$

Where s is a coefficient which depends on cement type.

S=0.20 for CEM 42.5 R, CEM 52.5 N and CEM 52.5 R

s= 0.25 for CEM 32.5 R and CEM 42.5 N

s= 0.38 for CEM 32.5 N

6.2 Application of Feret's model to the prediction of the compressive strength of CAFCC formulations

Here, the concern is to propose an analytical expression of the strength of the binder at 28 days σ_{L28} involved in relation of Feret for CAFFC formulations. For that purpose, a validation of the Feret's model is first proposed on a concrete formulation made with only Ordinary Portland Cement and mixed with a water/cement mass ratio near 0.6.

According to equation 1, the optimum volume of cement involved in the formulation of $1m^3$ of fresh concrete is equal 0.118 m^3. It corresponds to a mass of 357 kg according to the density of the cement used. The mass of water required with respect to the water/cement mass ratio is equal to 197 kg and corresponds to a volume of 0.197 m^3. Finally, the volume of entrained air is equal to 0.007 m^3 according to equation 2 and given that the volumetric ratio v_s / v_s + v_g is equal to 0.48. The compressive strength value obtained from Feret's model, *i.e.* 38.3 MPa, is very close to that measured experimentally, *i.e*. 38.5 MPa. The model is thus validated on concrete formulation prepared with OPC.

In order to establish the analytical expression of σ_{L28}, more specifically the expression of the coefficient ξ for concretes incorporating AFCC as given by equation 7, the same calculation method is applied to the three concrete formulations considered in this study. Results obtained are recorded in **Table 6** and compared with experimental values. From this comparison shown in **Figure 12**, the evolution of the coefficient ξ can be represented with an exponential law as given by equation (10). The regression coefficient R^2 is equal to 0.97.

Table 6. *Calculation of compressive strength values at 28 days from Feret's model for different substitution rates of cement by AFFC*

Substitution rate of cement (%)	0	5	10	20
v_b (m^3)	**0.118**			
v_w (m^3)	0.197	0.193	0.189	0.181
v_a (m^3)	0.007			
fcm_{28} (MPa) (Feret's model)	38.3	40.2	41.2	43.4
fcm_{28} (MPa) (experimental results)	38.5	37.8	31.5	27.1

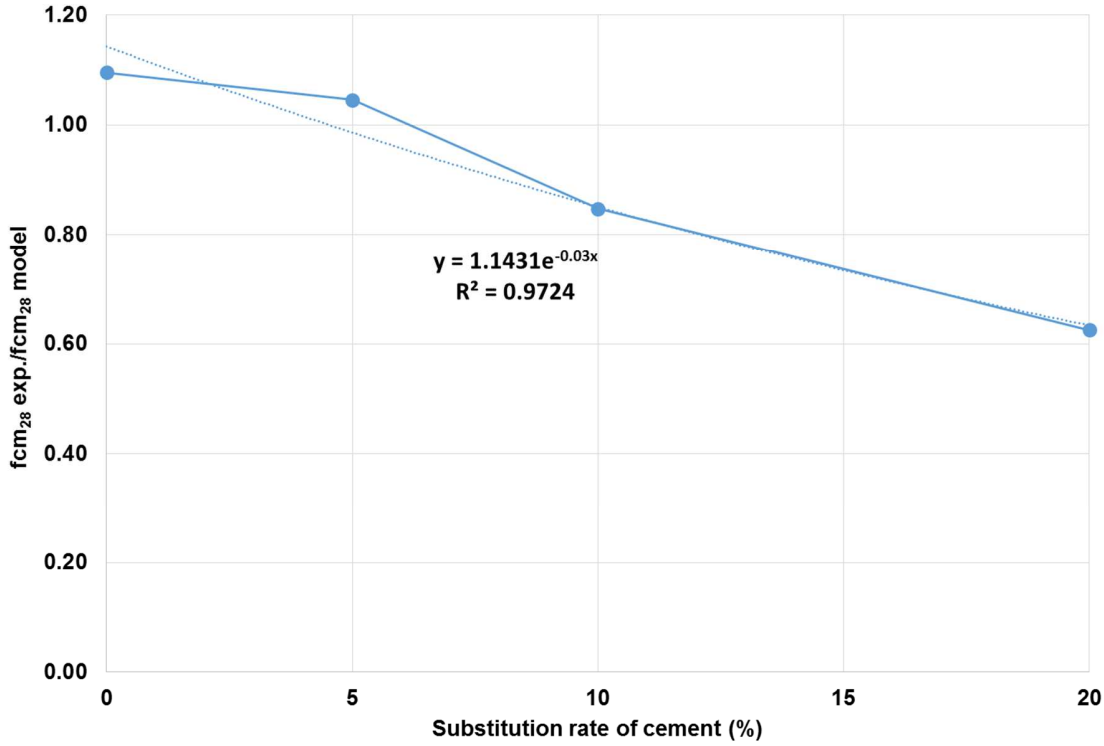

Figure 12*. Comparison between experimental compressive strength values at 28 days and compressive strength values at 28 days obtained from Feret's model for CAFCC formulations*

$$\xi(f) = 1.143 \times exp(-0.03f) \quad (10)$$

Where f (%) is the substitution rate of cement by AFCC.

Let us now compare the experimental evolution of the compressive strength in time, at 14 and 90 days respectively, with that provided by Eurocode 2 (equation 8). The value of the parameter s is equal to 0.2 because the cement used is a CEM I 52.5 R. According to results recorded in **Table 7**, Eurocode 2

reproduces in a satisfactory way the evolution of compressive strength obtained at 14 days but slightly underestimates that obtained at 90 days. It can be deduced that the model proposed by Eurocode 2 is appropriate to estimate the evolution in time of compressive strength of CAFCC formulations.

Table 7*. Comparison between experimental and calculated evolution with time of compressive strength values for CAFCC formulations*

Substitution rate of cement (%)	**0**	**5**	**10**	**20**
Compressive strength at 14 days (model) (MPa)	**36.9**	**32.6**	**28.9**	**25**
Compressive strength at 14 days (experimental) (MPa)	-	32.9	26.8	23.8
Compressive strength at 90 days (model) (MPa)	**43.8**	**38.7**	**34.3**	**29.6**
Compressive strength at 90 days (experimental) (MPa)	-	40.4	38.3	33.7

7. CONCLUSIONS AND FUTURE WORKS

From the experimental results and their analysis, the following conclusions can be drawn:
-The partial substitution of cement with fiber-cement causes an increase in water porosity. This is due to the drop in the density of the binder when increasing the substitution rate of cement. As consequence of the reduction in the mass of cement (replaced by AFFC), the mass of water is reduced too because of the constant water to binder mass ratio. The volume of cement hydration products for a given volume of concrete becomes thus lower when increasing the substitution rate of cement (low hydration potential of AFCC) and results in the formation of more capillary voids which is responsible for the increase in the water porosity. In terms of gas permeability, the replacement of cement by AFCC first leads to a decrease in permeability for substitution rates of cement up to 10%. In fact, the created capillary voids are not interconnected enough to form percolation paths for gas flow. However, for higher rates of substitution, *i.e.* between 10% and 20%, it can be observed that water porosity and gas permeability of CAFCC formulations evolve in the same way. This suggests that beyond a threshold value of substitution rate corresponding to 10%, the created capillary voids become increasingly interconnected, promoting the percolation of gas through the material.
-The replacement of cement by LF leads to an increase in water porosity up to a substitution rate of 10%. Indeed, a lower volume of cement hydration products is also formed for a given volume of concrete, resulting in the creation of more capillary voids. However, a decrease in water porosity is observed for substitution rates ranged between 10% and 20%. This can be explained by the formation of monocarboaluminate produced by the transformation of monosulfoaluminate observed experimentally and also reported in the literature. In terms of gas permeability, the replacement of cement by LF first leads to an increase in permeability for substitution rates of cement up to 5% followed by a decrease for higher rates of substitution. This result is consistent with the formation of monocarboaluminates in CLF formulations, which are certainly responsible for the progressive reduction of the percolation paths. For substitution rates ranged between 5 and 10%, the drop in gas permeability is accompanied with an increase in water porosity due to the fact that the production of monocarboaluminates is compensated

by the creation of capillary voids. These compensating effects become less pronounced from a threshold value of substitution rate (equal to 10%), for which water porosity and gas permeability evolve in the same way.
-From mechanical point of view, the partial replacement of cement with fiber-cement or limestone filler induces a decrease in compressive strength as the substitution rate of cement increases as a consequence of the creation of capillary voids. For CLF formulations, the formation of monocarboaluminates does not contribute to improve the compressive strength despite the refinement of the porous structure.
Based on experimental results, a modified Feret's model has been proposed in this study to predict the compressive strength of CAFCC formulations at 28 days. The experimental evolution of compressive strength in time is reproduced in a satisfactory way by Eurocode 2 model.

Durability aspects, especially in aggressive environments, will be considered in a future work.

7. REFERENCES

[1] Damtoft J.S., Lukasik J., Herfort D., Sorrentino D., Gartner E.M., "Sustainable development and climate change initiatives", Cement and Concrete Research, Volume 38, Issue 2, 2008, Pages 115-127

[2] Crossin E., "The greenhouse gas implications of using ground granulated blast furnace slag as a cement substitute", Journal of Cleaner Production, Volume 95, 2015, Pages 101-108

[3] Gartner E., "Industrially interesting approaches to "low-CO2" cements", Cement and Concrete Research, Volume 34, Issue 9, 2004, Pages 1489-1498

[4] Yang K.-H., Jung Y.-B., Cho M.-S., Tae S.-H., "Effect of supplementary cementitious materials on reduction of CO_2 emissions from concrete", Journal of Cleaner Production, Volume 103, 2015, Pages 774-783

[5] Bui N.K., Satomi T., Takahashi H., "Influence of industrial by products and waste paper sludge ash on properties of recycles aggregate concrete", Journal of Cleaner Production, Volume 214, 2019, Pages 403-418.

[6] Duchesne J., Bérubé M. A., "Effect of supplementary cementing materials on the composition of cement hydration products", Advanced Cement Based Materials, Volume 2, Issue 2, 1995, Pages 43-52

[7] Mounanga P., Khokhar M.I.A., El Hachem R., Loukili A., (2011) Improvement of the early-age reactivity of fly ash and blast furnace slag cementitious systems using limestone filler, Mater Struct 44:437–453

[8] Menéndez G., Bonavetti V., Irassar E.F., "Strength development of ternary blended cement with limestone filler and blast-furnace slag", Cement and Concrete Composites, Volume 25, Issue 1, 2003, Pages 61-67

[9] Chen H., Soles J.A., Malhotra V.M., "Investigations of supplementary cementing materials for reducing alkali-aggregate reactions", Cement and Concrete Composites, Volume 15, Issues 1–2, 1993, Pages 75-84

[10] Papadakis V.G., "Effect of supplementary cementing materials on concrete resistance against carbonation and chloride ingress", Cement and Concrete Research, Volume 30, Issue 2, February 2000, Pages 291-299

[11] Duchesne J., Bérubé M.A., "The effectiveness of supplementary cementing materials in suppressing expansion due to ASR: Another look at the reaction mechanisms part 1: Concrete expansion and portlandite depletion", Cement and Concrete Research, Volume 24, Issue 1, 1994, Pages 73-82,

[12] Kandasamy S., Shehata M. H., "The capacity of ternary blends containing slag and high-calcium fly ash to mitigate alkali silica reaction", Cement and Concrete Composites, Volume 49, 2014, Pages 92-99

[13]: Colangelo F., Navarro T.G., Farina I., Petrillo A., "Comparative LCA of concrete with recycled aggregates: a circular economy mindset in Europe", The International Journal of Life Cycle Assessment, Issue 9, 2020. (DOI: 10.1007/s11367-020-01798-6)

[14] Bonavetti V., Donza H., Menéndez G., Cabrera O., Irassar E.F., "Limestone filler cement in low w/c concrete: A rational use of energy", Cement and Concrete Research, Volume 33, Issue 6, 2003, Pages 865-871

[15] Li G., Zhao X., "Properties of concrete incorporating fly ash and ground granulated blast-furnace slag", Cement and Concrete Composites, Volume 25, Issue 3, 2003, Pages 293-299

[16] Shariq M., Prasad J., Masood A., "Effect of GGBFS on time dependent compressive strength of concrete", Construction and Building Materials, Volume 24, Issue 8, 2010, Pages 1469-1478

[17] Anderson D., Roy A., Seals R.K., Cartledge F.K., Akhter H., Jones S.C., "A preliminary assessment of the use of an amorphous silica residual as a supplement ary cementing material", Cement and Concrete Research 30 (2000) pp. 437- 445

[18] Chao-Lung H., Anh-Tuan B. L., Chun-Tsun C., "Effect of rice husk ash on the strength and durability characteristics of concrete", Construction and Building Materials, Volume 25, Issue 9, 2011, Pages 3768-3772

[19] Jamil M., Kaish A.B.M.A., Raman S.N., Zain M.F.M., "Pozzolanic contribution of rice husk ash in cementitious system", Construction and Building Materials, Volume 47, 2013, Pages 588-593

[20] Lee T.-C., Li Z.-S., "Conditioned MSWI ash-slag-mix as a replacement for cement in cement mortar", Construction and Building Materials 24 (2010) 970–979

[21] Renato Steiner L., Bernardin A. M., Pelisser F., "Effectiveness of ceramic tile polishing residues as supplementary cementitious materials for cement mortars", Sustainable Materials and Technologies 4 (2015) Pages 30-35

[22] Quercia G., van der Putten J.J.G., Hüsken G., Brouwers H.J.H., "Photovoltaic's silica-rich waste sludge as supplementary cementitious material (SCM)", Cement and Concrete Research 54 (2013) 161–179

[23] Müller A., Schnellert T., Seidemann M. (2011) "Material utilization of fibre cement waste", ZKG Int 64:60–72

[24] Bouharoun S., Leklou N., Mounanga P., "Use of asbestos-free fiber-cement waste as a partial substitute of Portland cement in mortar", Materials and Structures, Vol. 48, 2015, pp. 1679-1687.

[25] Féret R., " Sur la compacité des mortiers hydrauliques ", Annales des Ponts et Chaussées, Série 7, Volume 4, 1892, Pages 5-164 (in French)

[26] NF EN 197-1 Cement - Part 1: Compositions. Specifications and Conformity Criteria for Common Cement, European Committee for Standardization, Brussels, (2000).

[27] Klemm D., Philipp B., Heinze T., Heinze U., Wagenknecht W., 'Comprehensive Cellulose Chemistry, Fundamentals and Analytical methods'. Volume 1, 1998.

[28] Dreux G., "Nouveau guide du béton", 3rd Edition, Eyrolles, Paris, 1981 (in French).

[29] Dreux G., **Festa J.**, "Nouveau guide du béton et de ses constituants", 8th Edition, Eyrolles, Paris, 1998, 416 pages (In French).

[30] Dupain R., Lanchon R., Saint-Arroman J. C., " Granulats, sols, ciments et bétons : caractérisation des matériaux de génie civil par les essais de laboratoire, Nouvelle édition conforme aux normes européennes, 3ème édition actualisée, Edition Casteilla, 2004

[31] NF P 18-452. Bétons – Mesure du Temps d'Ecoulement des Bétons et des Mortiers aux Maniabilimètres. AFNOR, (1988).

[32] NF EN 12390-3 : Testing hardened concrete - Part 3 : compressive strength of test specimens - Essais pour béton durci - Partie 3 : Résistance à la compression des éprouvettes (2019)

[33] NF P 15-433. Méthodes d'Essais des Ciments – Détermination du Retrait et du Gonflement. AFNOR, (1994).

[34] AFPC – AFREM. 11-12. Compte-Rendu des Journées Techniques. Durabilité des Bétons. Toulouse (1997) 125-134.

[35] NF P 18-414. Essais des Bétons – Essais Non Destructifs. Mesure de la Fréquence de Résonance Fondamentale. AFNOR, (1993).

[36] **H. Taylor**, Cement Chemistry, 2nd ed., Thomas Telford, London, 1997.

[37] **V. Baroghel-Bouny**, Caractérisation microstructurale et hydrique des pâtes de ciment et des bétons ordinaires et à très hautes performances. Thèse de doctorat, Ecole Nationale des Ponts et Chaussées, 1994.

[38] Balonis M., Glasser F.P., "The density of cement phases", Cement and Concrete Research, Volume 39, Issue 9, September 2009, Pages 733-739.

[39] Lothenbach B., Le Saout G., Gallucci E., Scrivener K. "Influence of limestone on the hydration of Portland cements". Cement and Concrete Research, Vol. 38, n°6, (2008), p. 848-860.

[40] Zajac M., Rossberg A., Le Saout G., Lothenbach B. "Influence of limestone and anhydrite on the hydration of Portland cements". Cement and Concrete Composites, Vol. 46, (2014), p. 99-108.

[41] Moon J., Yoon S., Wentzcovitch R.M., Monteiro P.J.M., "First principles elasticity of monocarboaluminates hydrates", American Mineralogist, Volume 99, 2014, Pages 1360-1368**.**

[42] NF EN 1992-1-1 Eurocode 2: Design of concrete structures- Part 1-1: General rules and rules for building, October 2005.